Supporting Information for

Ag_7TaSe_6: New Noncentrosymmetric Selenide with Fascinating "Three in One" Coordination Modes and Strong Second Harmonic Generation Response

Zhuang Li,[a,b,c] Shengzi Zhang,[a,c] Wenlong Yin,[d] Kaijin Kang,[d] Yangwu Guo,[a,b,c] Wenhao Xing,[a,b,c] Zheshuai Lin,[a] Jiyong Yao,*[a,b] Yicheng Wu[a,e]

[a] Beijing Center for Crystal Research and Development, Key Lab of Functional Crystals and Laser Technology, Technical Institute of Physics and Chemistry, Chinese Academy of Sciences, Beijing 100190, P. R. China, corresponding author: Jiyong Yao, E−mail: jyao@mail.ipc.ac.cn.

[b] Center of Materials Science and Optoelectronics Engineering，University of Chinese Academy of Sciences, Beijing 100049, P. R. China

[c] University of Chinese Academy of Sciences, Beijing 100049, P. R. China.

[d] Institute of Chemical Materials, China Academy of Engineering Physics, Mianyang 621900, People's Republic of China.

[e] Institute of Functional Crystal Materials, Tianjin University of Technology Tianjin 300384, P.R. China.

Experimental details

1. Synthesis

Ag (99.9%), Ta (99.99%) and Se (99.99%) were directly purchased from Sinopharm Chemical Reagent Co., Ltd. All manipulations were performed in an Ar−filled glovebox with H_2O and O_2 contents less than 0.1 ppm. Polycrystalline sample of Ag_7TaSe_6 was obtained by traditional solid state reaction in a stoichiometric mixture of Ag, Ta and Se. The raw materials were loaded into fused−silica tubes and then, the ampoules were flame−sealed under a high vacuum of 10−3 Pa. The tubes were then placed in a computer−controlled furnace and heated to 973 K within 24 h, left for 96 h and, finally, the furnace was turned off. Single crystals of Ag_7TaSe_6 were prepared through spontaneous crystallization. The reaction mixture of Ag, Ta and Se in a molar ratio of 7 : 1 : 6 was mixed and loaded into a fused−silica tube. Then the tube was flame−sealed and gradually heated to 1273 K in a computer−controlled horizontal furnace, kept for 96 h, and then slowly cooled at a rate of 3 K/h and finally cooled to room temperature by switching off the furnace. The product consists of hundreds of black block−shaped crystals. These small crystals were stable in air for more than a year by now. The EDX−equipped field emission scanning electron microscope (Hitachi S−4800) analysis on several small crystals confirmed the presence of Ag, Ta and Se in the molar ratio of approximately 7 : 1 : 6. Then a crystal with good morphology was manually selected for structure characterization.

2. Structure determination

Single crystal X−ray diffraction data were recorded on a Xcalibur Ecos diffractometer equipped with a graphite−monochromated Mo−K_α (λ = 0.71073 Å) radiation at 293 K. The structure was solved with direct method by SHELXS−97 and refined by the full matrix least squares on F^2 by SHELXL−97, respectively. The detailed crystallographic data were summarized in Table S1. The atomic coordinates, occupancy and equivalent displacement parameters are given in Table S2. The important bond lengths and angles are listed in Table S3.

3. Property Characterization

Powder X−ray Diffraction

The powder X−ray diffraction pattern of the as−obtained polycrystalline powder was performed at room temperature on a Bruker D8 Focus diffractometer with Cu K_α (λ = 1.5418 Å) radiation. The scanning step width of 0.1º and a fixed counting time 0.2 s/step were applied to record the patterns in the 2θ range of 10 – 70º.

Element Analysis

Elemental analysis of compositions of the single crystal was performed on an energy−dispersive X−ray (EDX)−equipped Hitachi S−4800 scanning electron microscopy (SEM) instrument.

Diffuse reflectance spectroscopy

A Cary 5000 UV−vis−NIR spectrophotometer with a diffuse reflectance accessory was used to measure the spectrum of Ag_7TaSe_6 and $BaSO_4$ (as a reference) in the range 200 nm (6.2 eV) to 2500 nm (0.496 eV).

Thermal Analysis

By applying the Labsys^{TM} TG−DTA16 (SETARAM) thermal analyzer equipped with the nitrogen flow at a rate of about 30 mL/min, the thermal stability of Ag_7TaSe_6 was investigated in detail. Appropriate amounts of the polycrystalline powder were thoroughly ground, then were placed in a silica tube (5 mm o.d. × 3 mm i.d.) and subsequently sealed under a high vacuum. The tube was heated from 373 to 1273 K and then cooled to room temperature with the heating/cooling rate both at 15 K min^{-1}.

SHG Measurement

The optical SHG response of Ag_7TaSe_6 was measured by means of the Kurtz–Perry method. The fundamental light was the 2090 nm light generated with a Q−switched Ho: Tm: Cr: YAG laser. The polycrystalline powder of Ag_7TaSe_6 was thoroughly ground and sieved into a series of distinct particle size ranges of 20 − 41, 41 − 74, 74 − 105, 105 − 150 and 150 − 200 μm, respectively, which were then pressed into a disk with diameter of 8 mm that was put between glass microscope slides and secured with tape in a 1 mm thick aluminum holder. Microcrystalline

$AgGaS_2$ was ground and sieved into the same particle size ranges as reference.

4. Computational methods

The first–principles calculations for Ag_7TaSe_6 were performed by CASTEP, a plane–wave pseudopotential total energy package based density functional theory (DFT). The functional developed by Perdew–Burke–Emzerhoff (PBE) functional within the generalized gradient approximation (GGA) form were adopted to describe the exchange–correlation energy. The optimized norm–conserving pseudopotentials in the Kleinman–Bylander form for all the elements are used to model the effective interaction between atom cores and valence electrons. And Ag $4p^{10}5s^1$, Ta $4p^65d^36s^2$, Se $4s_24p_4$, electrons were treated as valence electrons, allowing the adoption of a relatively small basis set without compromising the computational accuracy. The high kinetic energy cutoff 500 eV and dense 2×2×2 Monkhorst–Pack k–point meshes in the Brillouin zones were chosen for Ag_7TaSe_6. Our tests showed that the above computational set ups are sufficiently accurate for present purposes. It is well known that the energy band gaps calculated by standard DFT method are smaller than the measured values, due to the discontinuity of exchange–correlation energy. The scissor operators were adopted to shift all the conduction bands to match the calculated band gaps with the measured values. Based on the scissor–corrected electron band structure, the imaginary part of the dielectric function was calculated according to the electron transition from the valence bands (VB) to conduction band (CB). Consequently, the real part of the dielectric function is obtained by the Kramers–Kronig transform and the refractive index is determined. The SHG coefficients d_{ij} were obtained by the formula developed by Lin's group.

5. Figure S1

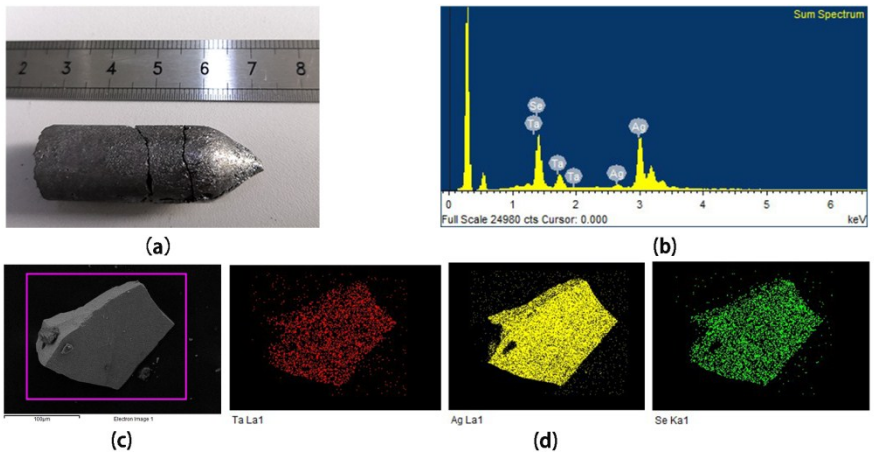

(a) Large size crystal of Ag_7TaSe_6 grown by Bridgman–Stockbarger method. (b) Elemental analysis of Ag_7TaSe_6 by EDX spectroscopy. (c) Scanning electron microscopy (SEM) image of Ag_7TaSe_6 grown by spontaneous crystallization. (d) Elemental distribution of the as−grown crystal (from left to right: Ta, Ag, Se).

6. Figure S2

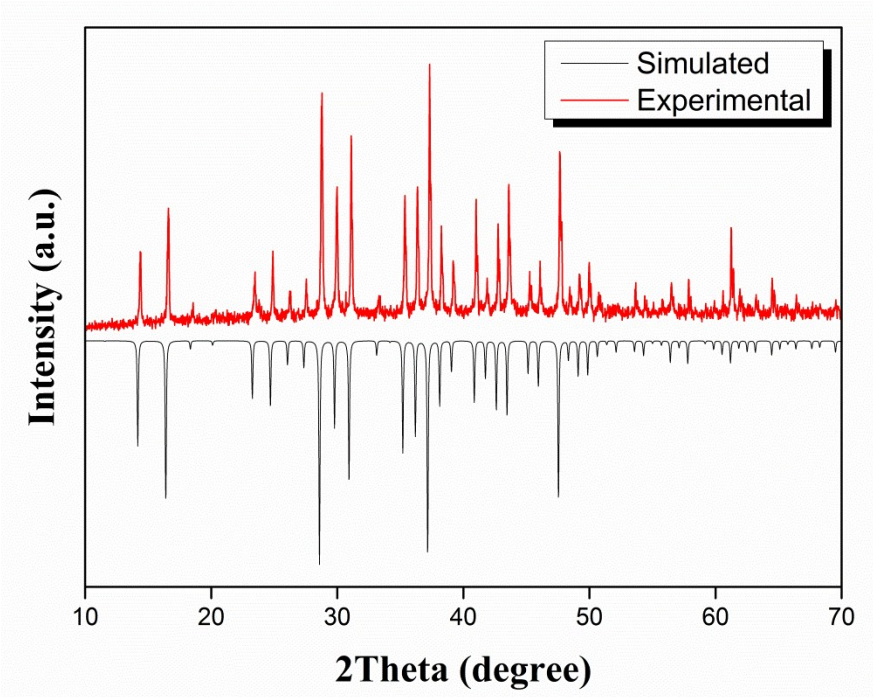

Experimental and simulated powder XRD patterns of Ag_7TaSe_6.

7. Figure S3

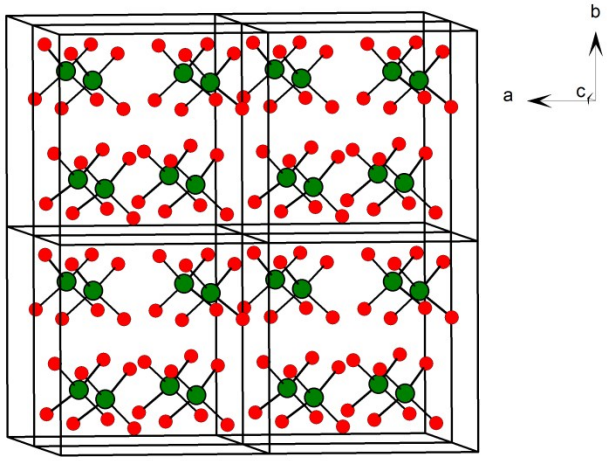

Macroscopic packing of $TaSe_4$ tetrahedra in the structure

8. Table S1 Crystallographic data and structure refinement for Ag_7TaSe_6.

Empirical formula	Ag_7TaSe_6
Formula weight	1409.80
Space group	$P2_13$
a/Å	10.809(2)
b/Å	10.809 (2)
c/Å	10.809 (2)
α/°	90.00
β/°	90.00
γ/°	90.00
V/Å^3	1262.9(4)
Z	4
ρ_{calc} g/cm^3	7.415
μ/mm^{-1}	36.482
F(000)	2424.0
Radiation	MoKα (λ = 0.71073 Å)
2θ range for data collection/°	5.32 to 54.8
Index ranges	$-14 \le h \le 7$, $-13 \le k \le 14$, $-12 \le l \le 11$
Reflections collected	4887
Independent reflections	954 [R_{int} = 0.0641]
Data/restraints/parameters	954/0/45
GOF on F^2	1.239
Final R indexes [I>=2σ (I)]	R_1 = 0.0292, wR_2 = 0.0767
Final R indexes [all data]	R_1 = 0.0292, wR_2 = 0.0767

9. Table S2 Fractional atomic coordinates (×10^4) and equivalent isotropic displacement

parameters ($Å^2×10^3$) for Ag_7TaSe_6. U_{eq} is defined as 1/3 of of the trace of the orthogonalized U_{ij} tensor.

Atom	x	y	z	Wyckoffsite	U(eq)
Ta1	−2463.3(3)	2536.7(3)	−7536.7(3)	4a	4.7(2)
Ag1	−7307.3(8)	−2586.3(8)	−10278.8(7)	12b	19.9(2)
Ag2	−4819.6(7)	1467.1(8)	−13208.2(8)	12b	17.9(2)
Ag3	−9016.7(8)	−9016.7(8)	983.3(8)	4a	30.9(4)
Se1	−3664.5(9)	1199.7(9)	−8904.8(9)	12b	9.7(2)
Se2	−2325.0(9)	−2675.0(9)	−7325.0(9)	4a	7.0(3)
Se3	−353.1(8)	−353.1(8)	−10353.1(8)	4a	9.9(3)
Se4	−8842.7(9)	−1157.3(9)	−6157.3(9)	4a	8.3(3)

10. Table S3 Selected bond lengths (Å) and angles (°) for Ag_7TaSe_6.

Ta1−Se1	2.4416(13)	$Se1^{\#1}$−Ta1−$Se1^{\#2}$	111.46(2)
Ta1−$Se1^{\#1}$	2.4416(13)	Se1−Ta1−$Se4^{\#3}$	107.40(3)
Ta1−$Se1^{\#2}$	2.4416(13)	$Se1^{\#1}$−Ta1−$Se4^{\#3}$	107.40(3)
Ta1−$Se4^{\#3}$	2.4451(19)	$Se1^{\#2}$−Ta1−$Se4^{\#3}$	107.40(3)
Ag1−$Se2^{\#9}$	2.6055(15)	$Se2^{\#9}$−Ag1−$Se1^{\#10}$	130.42(5)
Ag1−$Se1^{\#10}$	2.6256(13)	$Se2^{\#9}$−Ag1−$Se1^{\#11}$	126.13(5)
Ag1−$Se1^{\#11}$	2.6600(14)	$Se1^{\#10}$−Ag1−$Se1^{\#11}$	99.54(6)
Ag2−$Se3^{\#14}$	2.6191(10)	$Se3^{\#14}$−Ag2−$Se4^{\#15}$	135.77(5)
Ag2−$Se4^{\#15}$	2.6678(10)	$Se3^{\#14}$−Ag2−$Se1^{\#16}$	102.78(4)
Ag2−$Se1^{\#16}$	2.8200(14)	$Se4^{\#15}$−Ag2−$Se1^{\#16}$	91.68(5)
Ag2−$Se2^{\#14}$	2.8266(10)	$Se3^{\#14}$−Ag2−$Se2^{\#14}$	116.93(5)
Ag3−$Se3^{\#20}$	2.502(2)	$Se4^{\#15}$−Ag2−$Se2^{\#14}$	102.81(4)
Ag3−$Se2^{\#21}$	2.512(2)	$Se1^{\#16}$−Ag2−$Se2^{\#14}$	95.08(4)
Se1−Ta1−$Se1^{\#1}$	111.46(2)	$Se3^{\#20}$−Ag3−$Se2^{\#21}$	180.00(4)
Se1−Ta1−$Se1^{\#2}$	111.46(2)		